

Calculation of Landau levels in semiconductor quantum dots in a high magnetic field and at a high optical excitation

S. Nomura*

*The Institute of Physical and Chemical Research (RIKEN), Hirosawa, Wako-shi, Saitama, Japan
and Department of Solid State Physics and Nanometer Structure Consortium, Lund University, S-221 00 Lund, Sweden*

L. Samuelson

*Department of Solid State Physics and Nanometer Structure Consortium, Lund University, S221 00 Lund, Sweden
and The Institute of Physical and Chemical Research (RIKEN), Hirosawa, Wako-shi, Saitama, Japan*

C. Pryor and M.-E. Pistol

Department of Solid State Physics and Nanometer Structure Consortium, Lund University, S-221 00 Lund, Sweden

M. Stopa

The Institute of Physical and Chemical Research (RIKEN), Hirosawa, Wako-shi, Saitama, Japan

K. Uchida and N. Miura

Institute for Solid State Physics, University of Tokyo, Roppongi, Minato-ku, Tokyo, Japan

T. Sugano

The Institute of Physical and Chemical Research (RIKEN), Hirosawa, Wako-shi, Saitama, Japan

Y. Aoyagi

*The Institute of Physical and Chemical Research (RIKEN), Hirosawa, Wako-shi, Saitama, Japan
and Department of Solid State Physics and Nanometer Structure Consortium, Lund University, S-221 00 Lund, Sweden*

(Received 4 December 1997; revised manuscript received 28 April 1998)

Landau-level formations are studied theoretically for highly optically populated InP strained self-organized quantum dots for magnetic fields below 45 T. A self-consistent Hartree calculation is performed in real space with the higher-order finite difference method. A transition of the discrete states due to a potential confinement at 0 T to Landau-level-like structures for high magnetic fields is demonstrated. [S0163-1829(98)07435-9]

High magnetic-field effects in quantum dots (QDs),¹ are interesting because two limiting cases are realized by changing magnetic-field strength. At 0 T, discrete electronic states are formed by geometrical confinement by a QD potential structure, while at the high-field limit, magnetic confinement dominates over the potential confinement, forming electronic states with level spacings determined by a cyclotron motion of electrons.

In this paper, we consider the intermediate case, where both potential and magnetic confinement play roles in determining electronic states. We use a numerical method to explain previously observed Landau-level-like structures (LLSs) in photoluminescence (PL) spectra of InP/In_xGa_{1-x}P ($x=0.5$) strained QDs under high optical excitation conditions.² The electron-hole system in the QD is modeled as realistically as possible to reproduce the experimental conditions, in the framework of the Luttinger Hamiltonian with deformational coupling to strain fields. A higher-order finite difference method is used for calculating the electron and hole states.

Magnetic-field effects in QDs, using a quadratic confinement potential, has been done in Refs. 3–9. However, there are only a few reports¹⁰ on QDs with a square confinement potential in the presence of many electrons and holes per dot.

In this paper, we present theoretical calculations of LLS in QDs at high carrier density and in high magnetic fields.

Our results show that for increasing magnetic field, about 100 excited states in QDs evolve from discrete states at 0 T to LLSs at high magnetic fields. This effect is an interplay between the external magnetic field, the built-in strain field, the static confinement potential, and the Coulomb interaction between electrons and holes.

We treat the electrons and holes in a QD by a self-consistent Hartree calculation.^{10,11} The model Hamiltonians are

$$\mathcal{H}_e = \mathcal{H}_e^0(\mathbf{H}, e_{ij}) + V_H(\mathbf{r}) + V_e^0(\mathbf{r}) \quad (1)$$

and

$$\mathcal{H}_h = \mathcal{H}_h^0(\mathbf{H}, e_{ij}) - V_H(\mathbf{r}) + V_h^0(\mathbf{r}), \quad (2)$$

respectively. $\mathcal{H}_e^0(\mathbf{H}, e_{ij})$ and $\mathcal{H}_h^0(\mathbf{H}, e_{ij})$ are noninteracting single-particle Hamiltonians for an electron and a hole with terms depending on the external magnetic field \mathbf{H} and the strain tensor elements e_{ij} ,^{12–14} $V_H(\mathbf{r})$ is the Hartree term, and $V_e^0(\mathbf{r})$ and $V_h^0(\mathbf{r})$ are the bare confinement potentials for an electron and a hole, respectively. Realistic bare confinement potentials are considered in the calculation to reproduce the experiment in literature.² The geometry of our simulated InP QD is shown in Fig. 1(a). In the following we only discuss this fully developed QD, while there is a population of partially formed smaller QDs. The magnetic field \mathbf{H}

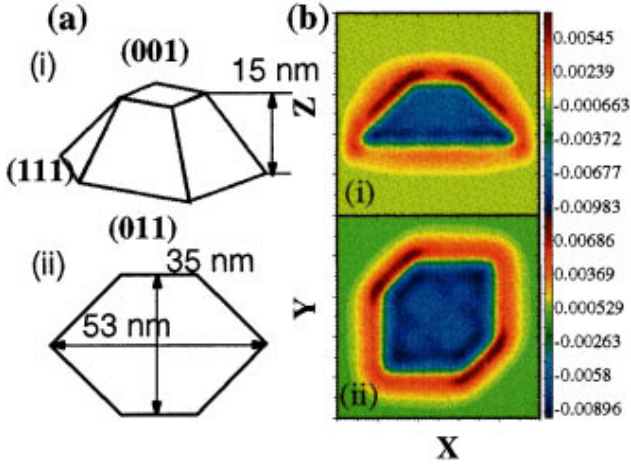


FIG. 1. (Color) (a) Perspective (i) and bottom (ii) views of the shape of a calculated InP QD. (b) Calculated charge density plots for vertical (i) and horizontal (ii) cross-sectional views of a QD at 0 T for $N_S=92$.

is taken to be parallel to the z direction. The Landau gauge $\mathbf{A}=(0,Hx,0)$ was used. The strain tensor elements e_{ij} were obtained using finite difference method. We used a cubic grid for the strain fields on the same grids that were used for the electronic structure.^{15,16} A linear deformational potential coupling of the strain fields to the electrons and holes was used. The valence-band mixing effect was considered by a 4×4 Luttinger Hamiltonian. The Hartree potential is given by

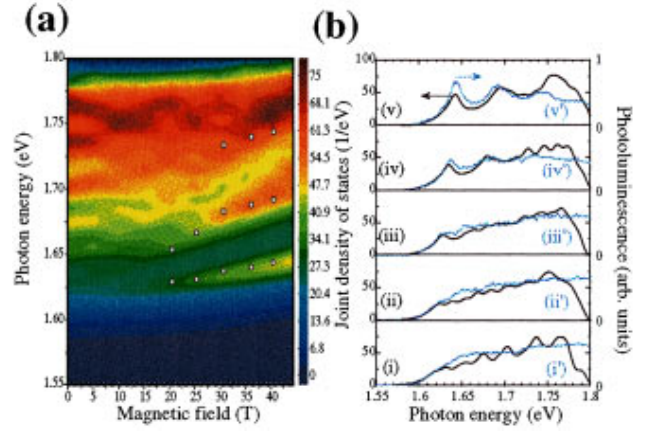


FIG. 3. (Color) (a) Contour plot of JDOS for $N_S=92$. Experimental results from Ref. 2 are also shown. (open circles). (b) JDOS at (i) 0 T, (ii) 10 T, (iii) 20 T, (iv) 30 T, and (v) 40 T for $N_S=92$. Zero points of the y axis are shifted as shown by the horizontal lines. The photon energy is shifted 120 meV lower for the purpose of comparison with the experimental results from Ref. 2 shown (blue dots) at (i') 0 T, (ii') 10.2 T, (iii') 20.8 T, (iv') 31.4 T, and (v') 40.9 T.

$$V_H(\mathbf{r}) = e^2 / (\epsilon \epsilon_0) \int d^3 \mathbf{r}' [n_e(\mathbf{r}') - n_h(\mathbf{r}')] / |\mathbf{r} - \mathbf{r}'|, \quad (3)$$

where $n_e(\mathbf{r})$ and $n_h(\mathbf{r})$ are the electron and hole densities.

The strained conduction-band offset was assumed to be 0.23 eV which has been experimentally determined by deep-level transient spectroscopy.¹⁷ Since the QDs are highly strained, the conduction-band minimum is 0.25 eV higher than in unstrained InP. Thus a bare conduction-band offset of 0.48 eV is used for $V_e^0(\mathbf{r})$. The composition of GaInP may also vary giving a change in the strained conduction-band offset of 0.23 eV. This effect is considered to be negligible though, since no fluctuations in the band-gap emission energy was observed using microphotoluminescence with a

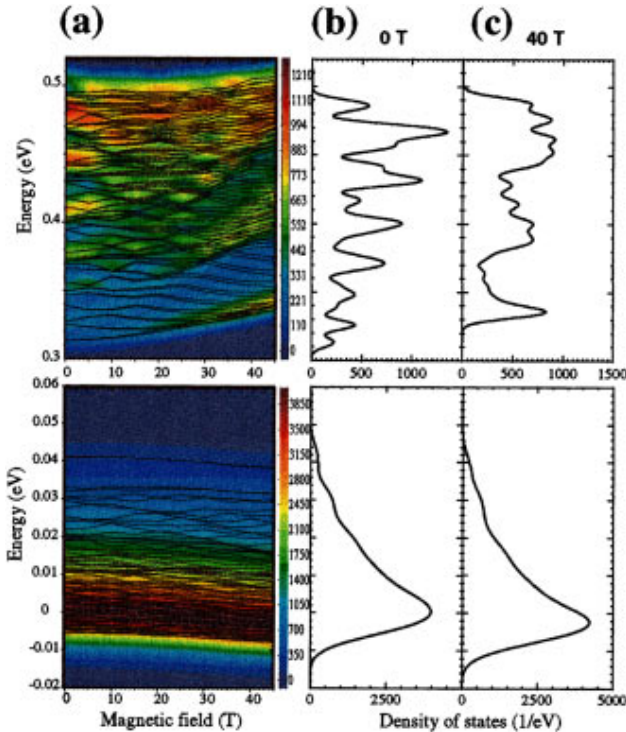


FIG. 2. (Color) (a) Magnetic-field dependence of the energy of states (solid curves) and a contour plot of DOS (background in color), and DOS at (b) 0 T and (c) 40 T of the electron (above) and hole (below) for $N_S=92$. The energy axis of the hole is taken to be negative.

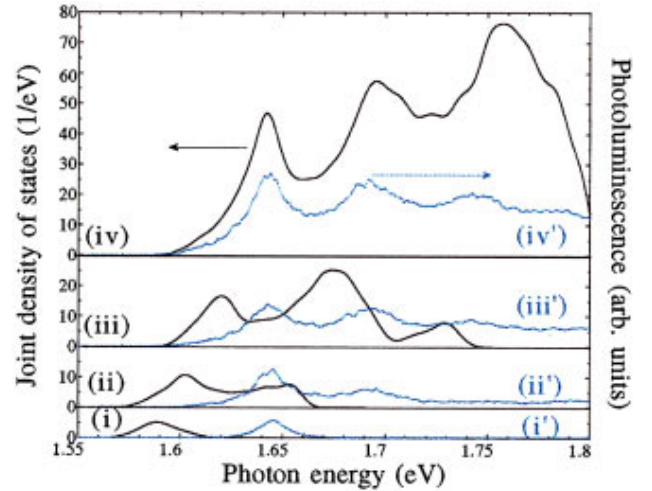


FIG. 4. (Color) JDOS at 40 T for $N_S=(i)$ 12, (ii) 23, (iii) 46, and (iv) 92 are shown (black dots). The photon energy is shifted 120 meV lower for the purpose of comparison with the experimental results from Ref. 2 shown (blue dots) for incident excitation power densities of (i') 90 W/cm² at $\lambda=488$ nm, (ii') 90, (iii') 180, and (iv') 360 W/cm² at $\lambda=514.5$ nm.

spatial resolution of about $1 \mu\text{m}$.¹⁸ The values for the deformational potentials were used from Ref. 16. Material parameters used in the calculation are $E_g=1.424$ (1.944) eV; $m_e=0.079$ (0.079) m_0 ; $g_c=1.31$ (1.31); $\gamma_1=4.58$ (4.58); $\gamma_2=1.32$ (1.32); $\gamma_3=2.00$ (2.00); $\kappa=0.66$ (0.66); $\varepsilon=12.61$ (12.61); $a_c=-5.1$ (-5.1) eV; $a_v=2.9$ (2.9) eV; $b=-2.0$ (-2.0) eV; $d=-5.0$ (-5.0) eV; $a_0=0.58687$ (0.56532) nm, $C_{xxx}=10.22$ (12.17) $\times 10^{11}$ dyn/cm²; $C_{xyy}=5.76$ (6.01) $\times 10^{11}$ dyn/cm²; $C_{xyxy}=4.60$ (5.82) $\times 10^{11}$ dyn/cm² for InP (Ga_{0.5}In_{0.5}P). Some parameters are assumed to be the same for InP and Ga_{0.5}In_{0.5}P for simplicity.

The coupled Schrödinger-Poisson equations [Eqs. (1)–(3)] were solved iteratively. Typically 40 iteration loops were made to give convergence of the eigenenergies of less than 0.1 meV. The wave functions were obtained by a real-space higher-order finite difference method of order 4 for the kinetic operator expansion.¹⁹ A von Neumann boundary condition was used. The number of the grids was taken to be $51\times 51\times 39$ and $70\times 70\times 49$ for the Schrödinger and Poisson equations, respectively, and the accuracy of the eigenenergies better than 0.1 meV were obtained. The grid spacings were fixed to 0.9375 nm for the former, and varied from 0.9375 nm inside and near the QD to 18.75 nm in the region far from the QD where spatial variation of the Hartree potential is small for the latter. Both the number of electrons and holes in a QD were fixed to N_S .

The calculated charge density shown in Fig. 1(b) for vertical (i) and for horizontal (ii) cross-sectional views, reveals that the QD is spatially type II, i.e., electrons inside a QD surrounded by holes partially outside the QD. The electron-hole recombination is nevertheless quite high, with a recombination time of about 1 ns.²⁰ Because of the large strain fields, the average effective potential for a hole is raised more than 40 meV in a QD. The electron-hole Coulomb interaction attracts holes to the center of a QD; however, this effect is smaller than the strain-induced effective potential of about 130 meV near the highly strained region of the top of the QD.

Figure 2(a) shows the magnetic-field dependence of energies of the electrons for the case of $N_S=92$. N_S is determined by the condition such that the joint density of states (JDOSs) spectra agree with the experimental results² as will be shown later. The states are seen to converge to several ladderlike structures with increasing magnetic field, forming LLS in QDs. As shown in Fig. 2 there are energy levels between the LLSs in contrast to the situation in higher dimensional structures, which is caused by a distortion of the cyclotron orbitals by the lateral confinement potential. The energy levels approach to those of three dimensions (3D) in the limit of a high magnetic field, where confinement by the crystal potential is negligible.

The density of states (DOSs) shows more clearly the formation of the LLS as shown in Figs. 2(a), 2(b), and 2(c). Here, a Gaussian distribution with a full width at half maximum of 12 meV is assumed for each level to account for the inhomogeneous width due to the fluctuations in the height, the lengths of the long and short axis of about $\pm 10\%$, and a possible increase of the carrier temperature. The change in the broadening parameter gives rise to the partial change in the width of the LLS; however, the dominant part of the width is determined by the confinement potential as will be

discussed later. Calculations were made from 0 to 45 T in steps of 5 T, and linear interpolations were made for values in between. At 0 T the peaks in the DOS of the electrons correspond to the quantum-confined states in a QD as shown in Fig. 2(b). With an increase in the magnetic field, the spectrum at 0 T evolves continuously to nearly equidistant structures by the magnetic confinement, forming the LLS from the lower energy as shown in Fig. 2(a). The striking difference with the Landau levels in 2D or 3D is that the DOS between the LLSs is intrinsically not zero even without introducing the width. This can be seen in Figs. 2(a) and 2(c) for the electron, at around 0.37 and 0.43 eV. This is because both the magnetic confinement and the potential confinement affect the energy spectra at magnetic fields less than 45 T. Thus the change in the broadening parameter gives rise to a minor change in the width of the LLS. In the extreme limit of the large magnetic field, the DOS approaches to that of a 3D system.

The DOS of the holes shows no significant features at 0 and 40 T. The change in peak position in the DOS of the holes between 0 and 40 T is 2.8 meV, which is negligible in comparison with the change in energy of the electrons. This is due to the heavy mass of the holes in addition to the strain induced localization of the holes. Thus the hole states contribute only a broadening of the spectral width of 15–20 meV in the JDOS, calculated below.

Optical selection rules, which are important for models with high symmetry are relaxed in our case, due to the low symmetry of the QD and also due to the localization of holes around the QD, caused by the effective potential including the strain fields and the Hartree term. Hence the optical transition spectra can be approximated by the JDOS.

Figures 3(a) and 3(b) show the magnetic-field dependence of the calculated JDOS for the case of $N_S=92$. The photon energy is shifted 120 meV to lower energy, for the purpose of comparison with the experimental results. This shift is caused partly by the uncertainties of the values of deformational potentials, and partly by the overestimate of the positive shift by the Hartree potential. The quasicontinuum seen at low magnetic fields will at high magnetic fields be replaced by a LLS. Initially for a small magnetic field, LLSs are not evident, as in Fig. 3(b), (i) and (ii). The first and the second LLSs are beginning to be formed at 20–25 T, while the states with higher energies, which have larger confinement energies, are less affected by the magnetic field and remain QD-like, as shown in Fig. 3(b), (iii). Finally at 40 T, three LLSs are seen in Fig. 3(b), (v), showing the magnetic confinement is dominant in all the states within a QD for $N_S=92$.

PL spectra and their peak positions from Ref. 2 are also shown in Figs. 3(b) and 3(a), respectively. Our calculated results are seen to reproduce the results in Ref. 2 quite well, especially the peak profiles of the PL spectra, shown in Fig. 3(b), (iii)–(v).

Nonequidistant LLSs observed are also reproduced in Fig. 3(b), which is caused by the effective confinement potential due to $V_e^0(\mathbf{r})$, the Hartree potential, and the strain fields. This is one of the significant features of the LLSs in a QD with nonparabolic confinement potential as compared with the bulk, 2D, or a parabolically confined QD, where the energy spacings between Landau levels are equal.

Here two aspects of the approximations made in the calculation are noted. First the JDOS is plotted instead of the optical transition probability in Figs. 3(a) and 3(b). The JDOS spectra reproduce well the formation of peaks by magnetic fields, but fail to reproduce relative intensity of each peak. At 40 T the peak height of the lowest peak is smaller than the second and third lowest peaks in the calculation, while the lowest peak is larger than the second and third lowest peaks in the PL spectra at 40.9 T. The error in the relative intensity of these peaks is considered to be mainly due to the neglect of calculating the optical transition probabilities and partly due to the fluctuation in the number of electrons in each QD. Second, a parabolic dispersion is used for the electron calculation. The energy spacings between the first and second peaks, and between the second and third peaks in the JDOS spectra at 40 T are 53.5 and 62.0 meV, while the counterpart of them in the PL spectra at 40.9 T are 48 and 52 meV, respectively. The disagreement with the experiment is larger for the higher energy peaks as shown in Fig. 3(a). The overestimate of the energies of higher excited states in the calculation is due to the neglect of the nonparabolicity of the conduction band.

Figure 4 shows the N_S dependence of the calculated JDOS at 40 T. It is seen that the LLSs are successively occupied with increasing N_S . While the exchange and correlation terms are known to be important for a small number of electrons or holes in a QD,^{3,8} a good agreement between experiment² and calculation, shown in Fig. 4, is nevertheless obtained here. This agreement implies that the correlation and exchange terms play small roles at high carrier densities and high magnetic fields in these QDs. PL studies of single QDs have also demonstrated that many-particle effects in this material system are weak.¹⁸

The discrepancies that do exist, e.g., the shift of the spectra with increasing carrier density seen in the calculations, which are not observed experimentally,² are ascribed to exchange and correlation effects. The positive energy shift caused by the Hartree energy is considered to be partly canceled by the negative energy shift by the band-gap renormalization, due to the self-energy of the electrons and holes. Finally we note that due to the variation in the QD sizes and fluctuations in the composition in GaInP, it is not presently feasible to discuss finer spectral structures than those discussed in the present paper. With the micro-PL technique under high magnetic fields, more detailed comparison of the theory with experiments is expected to be made possible.

In summary, we have studied the energy levels in a QD as a function of a magnetic field. The evolution of LLS in a QD has been modeled using a self-consistent Hartree calculation with a realistic shape of the QDs including the strain field, which clearly shows how the discrete states at 0 T evolve into a LLS at 45 T. Contrary to 2D or 3D cases, only the first LLS is recognized for the low magnetic field, while the second and the third LLSs appear for higher magnetic fields in the calculated JDOS spectra, due to a competition between the cyclotron energy and the lateral confinement energy. The calculated JDOS spectra show nonequispaced LLSs, which are caused by the nonparabolic effective confinement potential due to the bare confinement potential, the Hartree potential and the strain fields.

We are grateful to D. Hessman, B. Kowalski, and P. Omling for useful discussions. Computational support by the Computer Center of RIKEN is also gratefully acknowledged. This work was partly supported by a Grant-in-Aid for Scientific Research from the Ministry of Education, Science, Sports, and Culture of Japan.

*FAX: +81-48-462-4659.

Electronic address: snomura@postman.riken.go.jp

¹See, for example, L. Banyai, and S. W. Koch, *Semiconductor Quantum Dots* (World Scientific, Singapore, 1993).

²S. Nomura *et al.*, Appl. Phys. Lett. **71**, 2316 (1997).

³P. A. Maksym and T. Chakraborty, Phys. Rev. Lett. **65**, 108 (1990).

⁴A. Kumar, S. E. Laux, and F. Stern, Phys. Rev. B **42**, 5166 (1990).

⁵P. Bakshi, D. A. Broido, and K. Kempa, Phys. Rev. B **42**, 7416 (1990).

⁶V. Halonen, T. Chakraborty, and P. Pietiläinen, Phys. Rev. B **45**, 5980 (1992).

⁷N. F. Johnson, Phys. Rev. B **46**, 2636 (1992).

⁸D. Pfannkuche, V. Gudmundsson, and P. A. Maksym, Phys. Rev. B **47**, 2244 (1993).

⁹A. Angelucci and A. Tagliacozzo, Phys. Rev. B **56**, R7088

(1997).

¹⁰M. P. Stopa, Phys. Rev. B **54**, 13 767 (1996).

¹¹S. Nomura *et al.*, Phys. Rev. B **57**, 2407 (1998).

¹²K. Cho, *Excitons*, Vol. 14 of *Springer Tracts in Modern Physics* (Springer-Verlag, Berlin, 1979).

¹³G. E. Pikus and G. L. Bir, Fiz. Tverd. Tela (Leningrad) **1**, 1624 (1959) [Sov. Phys. Solid State **1**, 1502 (1960)].

¹⁴S. Nomura, Y. Segawa, and T. Kobayashi, Phys. Rev. B **49**, 13 571 (1994).

¹⁵C. Pryor, M.-E. Pistol, and L. Samuelson, Phys. Rev. B **56**, 10 404 (1997).

¹⁶K. Nishi *et al.*, J. Appl. Phys. **76**, 7437 (1994).

¹⁷S. Anand *et al.*, Appl. Phys. Lett. **67**, 3016 (1995).

¹⁸D. Hessman *et al.*, Appl. Phys. Lett. **69**, 749 (1996).

¹⁹J. R. Chelikowsky, N. Troullier, and Y. Saad, Phys. Rev. Lett. **72**, 1240 (1994).

²⁰P. Castrillo *et al.*, Appl. Phys. Lett. **67**, 1905 (1995).